ELSEVIER

16 August 1999

PHYSICS LETTERS A

Physics Letters A 259 (1999) 240–245

www.elsevier.nl/locate/physleta

# Elementary chaotic flow

Stefan J. Linz [a], J.C. Sprott [b]

[a] *Theoretische Physik I, Institut für Physik, Universität Augsburg, D-86135 Augsburg, Germany*
[b] *Department of Physics, University of Wisconsin, Madison, WI 53706, USA*

Received 21 April 1999; received in revised form 27 June 1999; accepted 29 June 1999
Communicated by C.R. Doering

**Abstract**

Using an extensive numerical search for the simplest chaotic non-polynomial autonomous three-dimensional dynamical systems, we identify an elementary third-order diffential equation that contains only one control parameter and only one nonlinearity in the form of the modulus of the dynamical variable. We discuss general properties of this equation and the possibility of chaotic behavior in functionally closely related equations. Finally, we present its analytical solution in an algorithmic way. © 1999 Published by Elsevier Science B.V. All rights reserved.

*PACS:* 05.45.-a; 47.52.+j; 02.30.Hq
*Keywords:* Chaos; Jerk; Flow; Strange attractor; Differential equations; Fractal

Following the seminal studies of Lorenz [1] and Rössler [2], the investigation of the time evolution of dynamical systems [3] in physics has been preferentially focused on the exploration and understanding of aperiodic or chaotic behavior within the last decades. Although there is no commonly accepted definition of chaotic behavior, it is widely accepted [3] that (i) a non-periodic bounded long-time evolution of a time-continuous dynamical system leading to a strange attractor in its phase space and (ii) a sensitive dependence on the initial conditions being characterized by the appearance of at least one positive Lyapunov exponent are signatures of a chaotic dynamics. It is also well known [3] that the basic requirements for the appearance of chaotic behavior in autonomous time-continuous dynamical systems, $\dot{\boldsymbol{x}} = \boldsymbol{V}(\boldsymbol{x})$ with $\boldsymbol{x}(t) = (x_1(t), \ldots, x_n(t))$, are (i) a phase space dimension $n \geq 3$ and (ii) some sort of nonlinearity in the vector field $\boldsymbol{V}(\boldsymbol{x})$.

In spite of the major progress and deep insights in the mechanisms that underlie regular and chaotic dynamics obtained so far [3,4], there are still fundamental questions that are only partly solved. A particularly interesting problem is the following: What are the simplest functional forms of three-dimensional autonomous dynamical systems that still possess chaotic behavior at least for some ranges of the control parameters? Only recently has this question attracted interest. Using a numerical search for three-dimensional dynamical systems that have only quadratic nonlinearities, Sprott [5] was able to identify nineteen distinct vector fields that are all functionally more elementary than the Lorenz model [1] and the Rössler model [2] and still possess a chaotic


PII: S0375-9601(99)00450-8

dynamics. On the other hand, Zhang and Heidel [6] were able to show analytically that many classes of vector fields being even simpler that Sprott's models [5] cannot be chaotic.

Even more recently, further progress in this direction has been achieved by considering a restricted class of three-dimensional dynamical systems, so-called *jerky dynamics* [7–11]. These are ordinary differential equations in one scalar real dynamical variable $x(t)$ that are (i) of third order, (ii) explicit and (iii) autonomous. Therefore, their functional form reads $\dddot{x} = J(x, \dot{x}, \ddot{x})$ with $\dddot{x}$ being the jerk or, mechanically speaking, the rate of change of the acceleration and $J(x, \dot{x}, \ddot{x})$ being the jerk function. Under certain restrictions, a jerky dynamics can interpreted as the direct extension of a one-dimensional Newtonian dynamics to spatially non-local forces [10]. Nevertheless, the investigation of jerky dynamics goes far beyond strictly mechanical systems [12]. In particular, the following has been shown: (i) One single quadratic nonlinearity in the otherwise linear jerk function can already lead to chaotic behavior [7–9], (ii) the simplest polynomial chaotic jerk function [7,8] is determined by $J(x, \dot{x}, \ddot{x}) = -A\dot{x} + \dot{x}^2 - x$ with $2.017 \leq A \leq 2.057$. Jerky dynamics can be considered as the direct time-continuous counterpart to one-dimensional chaotic iterated maps [3] with Sprott's minimal polynomial chaotic jerky dynamics [7,8] as counterpart of the logistic map.

The purpose of this letter is threefold. First, we examine how far the functional form of the nonlinearity can be weakened without losing the chaotic behavior in jerky dynamics. Second, we identify the probably most elementary piecewise linear chaotic jerky dynamics, discuss some of its general properties and present its analytical solution. Third, we give insight why functionally closely related jerky dynamics cannot behave chaotically.

Obviously, the most elementary piecewise linear functional dependence, the modulus of the dependent variable, $|x(t)|$, or equivalently, the product of the dependent variable and its sign, $x(t)\,\mathrm{sgn}[x(t)]$, seems to be a reasonable candidate for a nonlinearity that might lead to a potentially chaotic jerky dynamics. This speculation is also supported by the aforementioned analogy of jerky dynamics and one-dimensional iterated maps since it is well known that the piecewise linear tent map [3] shows chaotic behavior. Therefore, one might suppose that e.g. the general class of jerky dynamics

$$\dddot{x} + A_1\ddot{x} + A_2\dot{x} + A_3|x| + A_4 = 0 \tag{1}$$

with $A_i$ $(i = 1,2,3,4)$ being control parameters might behave chaotically for suitably chosen control parameter values and initial conditions. Note that Eq. (1) differs from a linear jerky dynamics *only by the replacement* of $x(t)$ by its modulus and not by the addition of the nonlinearity.

Provided that $A_2$ is non-zero, a scaling of the time, $t \to |A_2|^{-1/2}t$, and the dynamical variable, $x \to |A_2|^{-3/2}A_4\,x$, can be used to eliminate two coefficients from Eq. (1). The resulting functional form reads $\dddot{x} + A\ddot{x} \pm \dot{x} + C|x| + 1 = 0$ where the plus sign (minus sign) holds for $A_2 > 0$ ($A_2 < 0$) and the entering coefficients are given by $A = A_1|A_2|^{-1/2}$ and $C = |A_2|^{-3/2}A_3\,\mathrm{sgn}(A_4)$.

Since there are no analytical criteria known to decide whether Eq. (1) possesses chaotic dynamics for some ranges of the control parameter and initial conditions, the verification of our speculation relies on a systematic numerical search using the methods developed in Ref. [5,7,8,13]. To find chaotic solutions, the space of control parameters and initial conditions has been scanned to find a positive Lyapunov exponent [14] in the long-time evolution of (1). This has been accompanied by a subsequent check of the fractal dimension of the attractor.

Although during this procedure many control parameter combinations of Eq. (1) with chaotic dynamics have been found, we focus here on one particularly interesting and elementary subsystem of (1). It is obtained by setting $A_1 = A$ and $A_2 = -A_3 = A_4 = 1$ and explicitly given by the following non-polynomial jerky dynamics

$$\dddot{x} + A\ddot{x} + \dot{x} - |x| + 1 = 0. \tag{2}$$

To verify the appearance of chaotic behavior for some parameter ranges of $A$, we show in Fig. 1 the bifurcation diagram of the long-time evolution of the successive local maxima of the solution $x(t)$ in the range $0.5 \leq A \leq 0.8$. As initial conditions, $x = \dot{x} = \ddot{x} = 0$ have been used. The Feigenbaum diagram clearly shows a period-doubling route to chaos when $A$ is lowered from 0.8 to 0.64085. For smaller values of

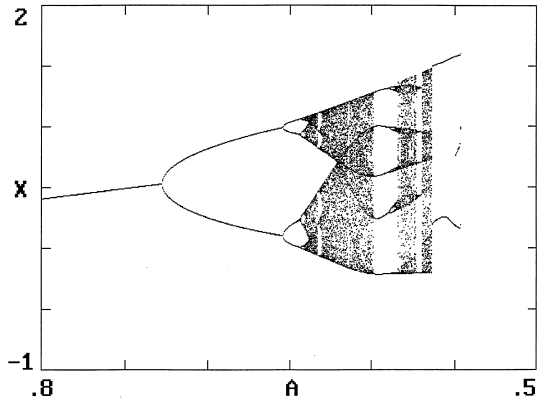


Fig. 1. Successive maxima of the long-time evolution of $x(t)$ generated by Eq. (2) as function of the control parameter $A$ in the range $0.5 \leq A \leq 0.8$. Initial conditions are given by $\ddot{x} = \dot{x} = x = 0$.

$A$, there is the typical chaotic band structure disrupted by the occurence of periodic windows. At $A \simeq 0.547$, the period-three dynamics becomes unstable and the long-time evolution of Eq. (2) diverges to infinity.

In Fig. 2, we show the largest Lyapunov exponent (LE) as a function of the control parameter $A$ in the same interval as in Fig. 1. Periodic (chaotic) dynamics corresponds to LE being equal to zero (positive). This substantiates that the band structure in Fig. 1 represents indeed regions of sensitive dependence on the initial conditions and, therefore, fulfils a signature of chaotic behavior.

Finally, as a representative example, we show in Fig. 3a stereoscopic view of the attractor for $A = 0.6$. This attractor possesses the typical Möbius-like structure known from the Rössler model [2] and also closely resembles the attractor of the minimal polynomial jerky dynamics [7]. For an animated rotational three-dimensional view of the chaotic attractor of Eq. (2) for $A = 0.6$, we refer to Ref. [15]. Moreover, the analysis of the Lyapunov spectrum shows that the Lyapunov or Kaplan–Yorke dimension [3] of the attractor at $A = 0.6$, $D_{\mathrm{KY}} = 2 - L_1/L_3$ with $L_1$ ($L_3$) being the largest (smallest) Lyapunov exponent, is given by 2.055. This substantiates that the attractor is a fractal.

In the remainder of the paper, we analyze Eq. (2) from the theoretical point of view. The only simple symmetry that Eq. (2) fulfils is the invariance with respect to the simultaneous transformation $x \to -x$, $t \to -t$, and $A \to -A$. Except for $A = 0$, Eq. (2) is not reversible.

Introducing $v = \dot{x}$ and $a = \dot{v} = \ddot{x}$, the nonpolynomial jerky dynamics (2) corresponds to a three-dimensional autonomous dynamical system $\dot{\boldsymbol{x}} = \boldsymbol{V}(\boldsymbol{x})$ with $\boldsymbol{x} = (x,v,a)^{\mathrm{T}}$ and a vector field $\boldsymbol{V}(\boldsymbol{x}) = (V_x,V_v,V_a)^{\mathrm{T}}$ that reads component-wise

$$\dot{x} = V_x = v$$

$$\dot{v} = V_v = a$$

$$\dot{a} = V_a = -Aa - v + |x| - 1. \tag{3}$$

Except for the component $\partial V_a/\partial x = \mathrm{sgn}(x)$ of the Jacobian matrix of the vector field, $\boldsymbol{J} = \partial \boldsymbol{V}(\boldsymbol{x})/\partial \boldsymbol{x}$ which is is discontinuous at $x = 0$, all other component of $\boldsymbol{J}$ are constant. Nevertheless, the vector field of the dynamical system (3) is still locally Lipschitzian at $x = 0$. According to the Picard–Lindelöf theorem [16], this guarantees existence and uniqueness of a continuous and differentiable solution $\boldsymbol{x}(t)$ as long as $\boldsymbol{x}(t)$ is bounded. This directly implies that $x(t)$, $\dot{x}(t)$, and $\ddot{x}(t)$ are also continuous and differentiable with respect to the time $t$ and therefore, the smoothness of the chaotic attractor shown in Fig. 3. Inspection of Eq. (2) shows that the jerk $\ddot{x}(t)$ is only continuous, and therefore, the rate of change of the jerk, $\dddot{x}(t)$ is discontinuous at values where $x(t)$ is zero.

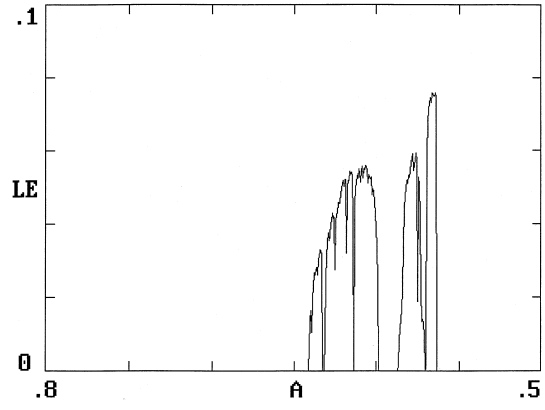


Fig. 2. Largest Lyapunov exponent (LE) as function of the control parameter $A$ in the same range as in Fig. 1.

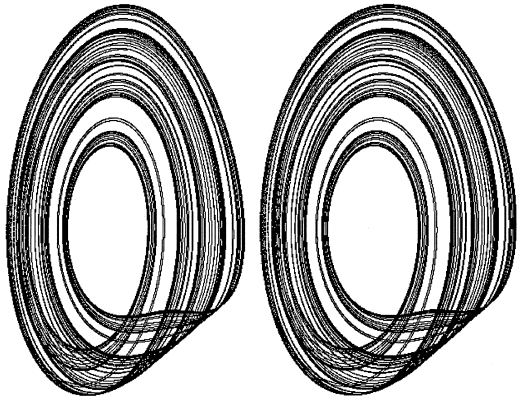

Fig. 3. Stereoscopic view of the strange attractor of Eq. (3) for the control parameter value $A = 0.6$ in order to obtain a three-dimensional impression. The corresponding Lyapunov exponents are given by $(L_1, L_2, L_3) = (0.035, 0, -0.635)$.

Integrating the model Eq. (2) with respect to time, it can be rewritten in the form of a *non-local oscillator*

$$\ddot{x} + A\dot{x} + x = \int^t \mathrm{d}\tau\big[|x(\tau)| - 1\big]. \tag{4}$$

Mechanically speaking, Eq. (4) can be interpreted in two ways: (i) As a damped harmonic oscillator being coupled by self-feedback $\int^t \mathrm{d}\tau\big[|x(\tau)| - 1\big]$ to its own dynamics or equivalently, (ii) as a one-dimensional Newtonian dynamics $\ddot{x} = F$ of a particle of unit mass where the force $F$ is an additive combination of $(\alpha)$ an instantaneous force $F_{\mathrm{inst}}$ that combines a frictional force $-A\dot{x}$ and the motion in a quadratic potential with $(\beta)$ a non-local force $F_{\mathrm{nl}} = \int^t \mathrm{d}\tau\big[|x(\tau)| - 1\big]$ or memory term that integrates over the positional history of the motion. Therefore, Eq. (2) represents a simple example of a Newtonian jerky dynamics [8–10].

In particular the second interpretation has important consequences for the possibility of chaotic behavior in jerky dynamics that are functionally closely related to (2). First, setting the additive constant in the jerky dynamics (2) to zero, $\dddot{x} + A\ddot{x} + \dot{x} = \int^t \mathrm{d}\tau |x(\tau)|$, chaotic dynamics cannot appear. This follows from the fact that the integrand of the memory term in Eq. (4) is positive semidefinite and, therefore, the memory term monotonically increases with time.

In the long time limit, the evolution of $x(t)$ eventually escapes to infinity. Second, the same argument also holds if the sign in front of the nonlinearity $|x|$ or the sign of the constant is inverted, $\ddot{x} + A\dot{x} + x = \pm \int^t \mathrm{d}\tau\big[|x(\tau)| + 1\big]$. In both cases chaotic behavior also cannot appear. This elucidates the importance of the non-zero constant in Eq. (2) and its sign for an aperiodic bounded dynamics. Moreover, one obtains as an implicit condition that bounded long-time dynamics cannot appear in Eq. (2) or (4) if the minimum of $|x(t)|$ is larger than unity.

The contraction rate in phase space of the dynamical system (3), $\Lambda = \partial_x \dot{x} + \partial_v \dot{v} + \partial_a \dot{a}$, equals the negative of the control parameter $-A$, and therefore, the model is globally dissipative for any positive $A$. Conversely, this also implies an unbounded or diverging dynamics of Eq. (2) for any negative $A$ and initial values being different from the fixed points. This narrows down the relevant control parameter range for bounded dynamics to $A > 0$. As can be seen from Fig. 1, however, this is not enough to guarantee boundedness of the time evolution of $x(t)$.

Obviously, Eq. (2) possesses two fixed points given by $x^\star = \pm 1$. To determine their stability, we consider deviations $u$ from these fixed points, $u = x - x^\star$, and rewrite Eq. (2) as $\dddot{u} + A\ddot{u} + \dot{u} - (x^\star + u)\mathrm{sgn}(x^\star + u) + 1 = 0$. If the modulus of $u$ is smaller than unity, we can replace $\mathrm{sgn}(x^\star + u)$ by $\mathrm{sgn}(x^\star)$. Using an ansatz $u(t) \propto \exp(\lambda t)$, the characteristic polynomial for the eigenvalues $\lambda$ is determined by $\lambda^3 + A\lambda^2 + \lambda - \mathrm{sgn}(x^\star) = 0$. Then, the Routh–Hurwitz criterion [1] [17] implies that the fixed point $x^\star = +1$ is unstable for any $A$, whereas the fixed point $x^\star = -1$ is stable for $A > 1$ and $|u| < 1$. At $A = 1$, the fixed point $x^\star = -1$ becomes unstable via a Hopf bifurcation since the corresponding eigenvalues are given by $\lambda_1 = -1$ and $\lambda_2 = -\lambda_3 = i$.

Based on the interpretation of Eq. (2) as a non-local oscillator, Eq. (4), we can provide a simple qualitative picture of the dynamical behavior as a function of $A$ as depicted in Fig. 1. Since the control parameter $A$ represents the damping constant of the non-local oscillator, we can roughly split the ranges of $A > 0$ into three parts. (i) For large damping,

[1] For a third order polynomial $\lambda^3 + a_1\lambda^2 + a_2\lambda + a_3 = 0$, the Routh–Hurwitz criterion states [17] states that the real parts of the roots $\lambda$ are negative if (and only if) the conditions $a_1 > 0$, $a_3 > 0$, and $a_1 a_2 - a_3 > 0$ are fulfilled.

$A > 1$, the oscillation amplitudes rapidly diminish and the memory term on the right hand side of Eq. (4) approaches quickly a constant. (ii) In the intermediate range $0.547 \leq A \leq 1$, the damping is too weak to force the memory term to approach a constant. Therefore, the memory term oscillates giving rise to the plentora of complicated bounded dynamical behavior seen in Fig. 1. (iii) For $A < 0.547$, the damping is too weak to keep the motion bounded. The memory term on the right hand side of Eq. (4) builds up and diverges to infinity.

As an aside, we note that replacing the nonlinearity $|x|$ by $x^2$ in Eq. (2), $\dddot{x} + A\ddot{x} + \dot{x} - x^2 + 1 = 0$, leads to a polynomial jerky dynamics that cannot show chaotic behavior for the initial conditions mentioned above. The most complex dynamics of this equation is a period-four limit cycle around $A = 1.125$ that is bordered by two period-two limit cycles. For $A$ smaller than about 1.1075, the dynamics is unbounded. Therefore, it is the algebraic weakness of the nonlinearity in Eq. (2) that gives rise to the complex dynamics depicted in Fig. 1.

Since Eq. (2) is piecewise linear, its exact solution can be obtained segment by segment for $x(t) < 0$ and $x(t) > 0$ combined with the appropriate matching conditions for $x(t) = 0$. The skeleton of the solution of Eq. (2) is determined by the solution of the linear equations

$$\dddot{x} + A\ddot{x} + \dot{x} \pm x + 1 = 0 \qquad (5)$$

where the *plus sign* in Eq. (5) applies if $x \leq 0$ and the *minus sign* if $x \geq 0$. The solutions of Eq. (5) read explicitly

$$x(t) = \pm(-1) + \sum_{k=1}^{3} C_{\pm}^{(k)} \mathrm{e}^{\rho_{\pm}^{(k)} t} \qquad (6)$$

where $C_{\pm}^{(k)}$ are constants that are determined by the initial conditions and $\rho_{\pm}^{(k)}$ the roots of the third-order polynomial $\rho_{\pm}^3 + A\rho_{\pm}^2 + \rho_{\pm} \pm 1 = 0$. The latter can be explicitly calculated for any given $A$ using Cardani's formula [2].

[2] The structure of the roots in the control parameter range $0 \leq A \leq 1$ is as follows. If $x(t) < 0$ [$x(t) > 0$], the roots are given by $\rho_+^{(1)} = \sigma_+^{(1)}$ [$\rho_-^{(1)} = \sigma_-^{(1)}$] and $\rho_+^{(2)} = \left(\rho_+^{(3)}\right)^* = \sigma_+^{(2)} + i\omega_+$ [$\rho_-^{(2)} = \left(\rho_-^{(3)}\right)^* = \sigma_-^{(2)} + i\omega_-$] where $\sigma_+^{(1)}$ [$\sigma_-^{(1)}$] is real and negative [positive], $\sigma_+^{(2)}$ [$\sigma_-^{(2)}$] real and positive [negative], and $\omega_+$ and $\omega_-$ real. Except for $A = 0$, the moduli of $\sigma_{\pm}^{(j)}$ ($j = 1,2$) and $\omega_{\pm}$ differ for $x(t) > 0$ and $x(t) < 0$.

The solution $x(t)$ of Eq. (2) can be expressed as

$$x(t) = \sum_{j=1}^{N} x_j(t)\Theta(t - t_{j-1})\left[1 - \Theta(t - t_j)\right] \qquad (7)$$

with $\Theta(\zeta)$ denoting the Heaviside function [$\Theta(\zeta) = 0$ (1) if $\zeta < 0$ ($\geq 0$)], $j = 1,2,\ldots$ the number of the segment, $x_j(t)$

the solution of the $j$-th segment, and $N$ the maximum number of segments. If the solution of Eq. (2) reaches the fixed point or is unbounded, $N$ is finite. For any other dynamical behavior, $N$ is infinite. The solution of the $j$-th segment, $x_j(t)$, for the time interval $t_{j-1} \leq t \leq t_j$ obeys $\dddot{x}_j + A\ddot{x}_j + \dot{x}_j + s(j)x_j + 1 = 0$ and is determined by

$$x_j(t) = s(j)(-1) + \sum_{k=1}^{3} C_{s(j)}^{(k)} \exp\left(\rho_{s(j)}^{(k)} t\right) \qquad (8)$$

with initial conditions $x_j(t_{j-1}) = x(0)$, $\dot{x}_j(t_{j-1}) = \dot{x}(0)$ $\ddot{x}_j(t_{j-1}) = \ddot{x}(0)$ if $j = 1$ and $x_j(t_{j-1}) = 0$, $\dot{x}_j(t_{j-1}) = \dot{x}_{j-1}(t_{j-1})$, $\ddot{x}_j(t_{j-1}) = \ddot{x}_{j-1}(t_{j-1})$ if $j = 2,3,\ldots$. The sign of the $j$-th segment, $s(j) = \pm$, generically switches from segment to segment, $s(j) = -s(j+1)$, and selects the relevant roots $\rho_{\pm}^{(k)}$ for the segment. The initial conditions determine $s(1)$. In particular, $s(1)$ equals $+$ $(-)$ if $x(0) < 0$ ($x(0) > 0$). For the special initial conditions $x(0) = \dot{x}(0) = \ddot{x}(0) = 0$, $s(1) = -$ applies. The coefficients $C_{s(j)}^{(k)}$ are given by the solution of the linear algebraic system

$$0 = s(j)(-1) + \sum_{k=1}^{3} C_{s(j)}^{(k)} \exp\left(\rho_{s(j)}^{(k)} t_{j-1}\right)$$

$$\dot{x}_j(t_{j-1}) = \sum_{k=1}^{3} \rho_{s(j)}^{(k)} C_{s(j)}^{(k)} \exp\left(\rho_{s(j)}^{(k)} t_{j-1}\right)$$

$$\ddot{x}_j(t_{j-1}) = \sum_{k=1}^{3} \left[\rho_{s(j)}^{(k)}\right]^2 C_{s(j)}^{(k)} \exp\left(\rho_{s(j)}^{(k)} t_{j-1}\right).$$

The $j$-th segment of the solution ends when the time $t_j$ given by $x_j(t_j) = 0$ has been reached. The time $t_j$ is determined by the smallest value of $t$ that is larger than $t_{j-1}$ and obeys the transcendental equation

$$0 = s(j)(-1) + \sum_{k=1}^{3} C_{s(j)}^{(k)} \exp\left(\rho_{s(j)}^{(k)} t_j\right). \qquad (9)$$

The values $x_j(t_j)$, $\dot{x}_j(t_j)$, and $\ddot{x}_j(t_j)$ determine the initial conditions for the solution segment $x_{j+1}$.

Despite the functional simplicity of Eq. (2), its algorithmically determined solution looks rather complicated and is not obvious that it leads to the

complex dynamical behavior depicted in Fig. 1. A more detailed analysis will be given elsewhere [18]. Here, we only note that $p$-periodic solutions ($p$ positive and integer) are determined by the condition $x_j(t) = x_{j+2p}(t - \tau_p)$ with $\tau_p = t_{j+2p-1} - t_{j-1}$ in the long time limit, whereas chaotic solutions do not reduplicate at all.

In conclusion, we have identified and partly analyzed the apparently most elementary piecewise linear jerky dynamics or three-dimensional dynamical system that still allows for a chaotic evolution in time for some control parameter ranges. This system can be considered as the time-continuous chaotic counterpart to the most elementary chaotic iterated map, the tent map [3]. The simplicity of this system invites electronic implementation using operational amplifiers and diodes. Such a circuit has been constructed and tested and behaves as predicted to within the precision of the electronic components (typically 10%) [15,19].

## Note added in proof

After the acceptance of this letter, we learned of a related study by A. Arneodo, P. Coullet, and C. Tresser [J. Stat. Phys. 27 (1982) 171]. Using Shil'nikov's theorem, these authors were able to prove that the differential equation $\dddot{x} + \beta\ddot{x} + \dot{x} = f(x)$ with the piecewise linear function $f(x) = 1 + ax$ if $x \le 0$ and $f(x) = 1 - \mu x$ if $x \ge 0$ satisfies the Shil'nikov conditions for appropriately chosen values of the three entering parameters $\beta = 0.3375$, $a = 0.633625$ and $\mu \simeq 2.158$. This study, however, did not deal with our more elementary case of a modulus nonlinearity, $a = \mu = 1$. It remains an open problem for future research whether the appearance of chaos in our system, Eq.(2), can also be more analytically motivated.

## References


[1] E.N. Lorenz, J. Atmos. Sci. 20 (1963) 130.
[2] O.E. Rössler, Phys. Lett. A 57 (1976) 397.
[3] For a review cf. E.A. Jackson, Perspectives in Nonlinear Dynamics, Vol. I and II (Cambridge Univ. Press, Cambridge, 1989); S.H. Strogatz, Nonlinear Dynamics and Chaos (Addison–Wesley, Reading, 1994): J. Argyris, G. Faust, M. Haase, An Exploration of Chaos (Springer, New York, 1996); H.G. Solari, M.A. Natiello, G.B. Mindlin, Nonlinear Dynamics (IOP Publ., Bristol, 1996).
[4] J.P. Eckmann, D. Ruelle, Rev. Mod. Phys. 57 (1985) 617; R. Gilmore, Rev. Mod. Phys. 70 (1998) 1455.
[5] J.C. Sprott, Phys. Rev. E 50 (1994) R647.
[6] Zhang Fu, J. Heidel, Nonlinearity 10 (1997) 1289.
[7] J.C. Sprott, Phys. Lett. A 228 (1997) 271.
[8] J.C. Sprott, Am. J. Phys. 65 (1997) 537.
[9] S.J. Linz, Am. J. Phys. 65 (1997) 523.
[10] S.J. Linz, Am. J. Phys. 66 (1998) 1109.
[11] R. Eichhorn, S.J. Linz, P. Hänggi, Phys. Rev. E 58 (1998) 7151.
[12] For a popular review on jerky dynamics cf. H.C. von Baeyer, The Sciences 38 (1998) 12.
[13] J.C. Sprott, Comput. Graphics 7 (1993) 325.
[14] G. Benettin, L. Galgani, A. Giorgilli, J.-M. Strelcyn, Meechanica 15 (1980) 21.
[15] http://sprott.physics.wisc.edu/chaos/abschaos.htm.
[16] L. Perko, Differential Equations and Dynamical Systems (2nd ed., Springer, New York, 1996).
[17] J.D. Murray, Mathematical Biology (2nd ed., Springer, Berlin, 1993).
[18] S.J. Linz, J.C. Sprott, in preparation.
[19] J.C. Sprott, to be published.